

## Impacts of cool roofs on urban heat island and air quality in Dhaka, Bangladesh: A case modeling study during a heat wave

Abeda Tabassum<sup>a</sup> , Kyeongjoo Park<sup>a</sup> , Seong-Ho Hong<sup>a</sup>, Jong-Jin Baik<sup>a,\*</sup>, Beom-Soon Han<sup>b</sup>

<sup>a</sup> School of Earth and Environmental Sciences, Seoul National University, Seoul, South Korea

<sup>b</sup> Department of Environmental Engineering, Inha University, South Korea

### ARTICLE INFO

#### Keywords:

Cool roof  
Urban heat island  
Air quality  
Urban breeze  
Dhaka  
Heat wave

### ABSTRACT

This study investigates the impacts of cool roofs on the urban heat island (UHI) and air quality in Dhaka, Bangladesh during an extreme heat wave event occurring in April 2021. A simulation with conventional roofs having an albedo of 0.2 and a simulation with cool roofs having an albedo of 0.8 are conducted using the Weather Research and Forecasting (WRF) model. Cool roofs reduce the 2-m temperature by 0.57 °C in the afternoon (1200–1700 LST) and cause the urban cool island in the daytime. In the afternoon, cool roofs reduce the planetary boundary layer height by 265 m and greatly suppress the urban breeze, reducing the 10-m wind speed by 0.8 m s<sup>-1</sup>. As a result, the near-surface passive tracer (carbon monoxide) concentration increases by 45 ppb (52 %) in the afternoon. Cool-roof effects on the UHI and air quality are overall more pronounced in hotter areas. Cool roofs lead to statistically significant decreases in Humidex (-0.19), discomfort index (0.22), and heat index (-0.36 °C) in the afternoon, but all indices remain within the same stress levels. This suggests that additional measures such as urban greenery and other climate-sensitive urban designs are required along with cool roofs for an effective mitigation of urban extreme heat in Dhaka.

### 1. Introduction

Due to the rapid urban expansion in recent decades, 56 % of the world population now lives in urban areas, and this number is estimated to reach 68 % by the end of 2050 (UN-Habitat, 2022). A renowned consequence of urbanization is the urban heat island (UHI), the urban areas exhibiting higher temperatures than their surrounding rural areas due to their impervious surfaces, reduced vegetation, and anthropogenic heat (Phelan et al., 2015). The UHI increases heat-related mortality (Ho et al., 2023), increases energy consumption (Santamouris et al., 2015), and may worsen air quality (Lai and Cheng, 2009). Moreover, the UHI can synergistically interact with heat waves, further increasing heat-related risks during heat waves (e.g., Li and Bou-Zeid, 2013). With continued urbanization and climate change, effective strategies for mitigating the UHI are necessary to reduce urban heat-related risks.

Numerous studies have been performed to seek effective strategies to mitigate the UHI. The most widely-recognized strategies to mitigate the UHI include cool roofs (Cao et al., 2015; Baniassadi et al., 2019; He et al., 2020; Baik et al., 2022; Rawat and Singh, 2022; Elnabawi et al., 2023; Reed and Sun, 2023), green roofs (Razzaghmanesh et al., 2016; Imran et al., 2018; Wang et al., 2022), and phase-changing materials (Roman

et al., 2016; Rawat et al., 2022). Cool roofs are shown to effectively mitigate the UHI, especially in the daytime (Li and Norford, 2016; Macintyre and Heaviside, 2019; Reed and Sun, 2023; Wang et al., 2023). Using high-resolution ensemble simulations during April–May in Singapore, Li and Norford (2016) showed a maximum reduction of 1.8 °C in UHI intensity at 1300 LST as the roof albedo increases from 0.20 to 0.88. Wang et al. (2023) performed numerical simulations during summer in the Pearl River Delta, China and showed a maximum reduction of 1.7 °C in UHI intensity as the roof albedo increases from 0.2 to 0.9. Reed and Sun (2023) conducted simulations of a heat wave in mid-July 2012 in the Kansas City metropolitan area, U.S. and showed that during the heat wave, cool roofs can reduce the UHI intensity by 0.64 °C.

While cool roofs are effective in mitigating the UHI, they can have adverse effects on air quality (Fallmann et al., 2016; Epstein et al., 2017; Falasca and Curci, 2018; Zhang et al., 2019; Han et al., 2020; Zhong et al., 2021; Park and Baik, 2024). Zhang et al. (2019) examined the effects of city-wide cool roof adoption on PM<sub>2.5</sub> concentration during June–July in Southern California, U.S. through simulations using a coupled meteorology–chemistry model, with roof albedo increasing from 0.10 to 0.90. They showed that the daily average PM<sub>2.5</sub>

\* Corresponding author. School of Earth and Environmental Sciences, Seoul National University, Seoul 08826, South Korea.

E-mail address: [jjaik@snu.ac.kr](mailto:jjaik@snu.ac.kr) (J.-J. Baik).

**Table 1**

Model setup and physics parameterizations for this study.

Simulation period	0600 LST April 24 – 0600 LST April 26, 2021
Horizontal grid size	27, 9, 1, and 0.333 km (domains 1, 2, 3, and 4)
Horizontal grid number	379 × 379
Vertical grid number	43
Initial/boundary conditions	ERA5 reanalysis (1-h intervals, $0.25^\circ \times 0.25^\circ$ resolution) (Hersbach et al., 2020)
Shortwave radiation	Dudhia shortwave scheme (Dudhia, 1989)
Longwave radiation	RRTM longwave scheme (Mlawer et al., 1997)
Planetary boundary layer	Yonsei University (YSU) scheme (Hong et al., 2006)
Surface layer	revised MM5 scheme (Jiménez et al., 2012)
Cumulus	Kain–Fritsch scheme (applied only in domain 1) (Kain, 2004)
Microphysics	WRF double moment 6-class microphysics scheme (Lim and Hong, 2010)
Land surface	unified Noah land surface model (Chen and Dudhia, 2001)
Urban surface	Seoul National University Urban Canopy Model (SNUUCM) (Ryu et al., 2011)

concentration in the region increases by  $0.85 \mu\text{g m}^{-3}$  and attributed this increase to the reduced ventilation that disrupts the mixing and transport of pollutants. Park and Baik (2024) performed two-dimensional idealized ensemble simulations to investigate the effects of increasing roof albedo on UHI intensity and air pollutant concentration and showed a 115 % increase in passive tracer concentration as the roof albedo increases from 0.20 to 0.65. Conversely, cool roofs also can have beneficial effects on air quality by reducing energy consumption and temperature-dependent chemical reactions (Akbari et al., 2001; Tou-chaei et al., 2016; Jandaghian and Akbari, 2018).

Dhaka, the capital of Bangladesh, is a tropical megacity with 10.3 million inhabitants (BBS, 2022). Dhaka has the tropical savannah climate in the Köppen-Geiger climate classification (Beck et al., 2018). Dhaka exhibits the hottest weather in the pre-monsoon season among the whole year, with a mean daily maximum temperature of  $\sim 34^\circ\text{C}$ . The rapid urbanization of Dhaka exposes the residents to great heat stress (Imran et al., 2021; Abrar et al., 2022), together with heat waves often occurring in this season (Nissan et al., 2017). Green roofs were studied as a mitigation measure for heat stress in Dhaka (Sultana et al., 2021; Bach et al., 2023). Meanwhile, cool roofs, another most widely adopted mitigation measure, have not been examined in Dhaka to the authors' knowledge. Given its considerable impacts reported for other cities (e.g., Santamouris, 2014), the cool-roof impacts on urban heat stress in Dhaka deserve detailed investigation. The urbanization of Dhaka causes air pollution problems as well as the heat-related risks; the annual mean  $\text{PM}_{10}$  concentration in Dhaka is  $155 \mu\text{g m}^{-3}$  (Rahman et al., 2019) which is about 10 times the air quality guideline level of World Health Organization (WHO, 2021). Considering the reported worsening of air quality due to cool roofs, the possible impacts of cool roofs on air quality in Dhaka need to be investigated in addition to its heat mitigation effects. The investigation can give implications for applicability of cool roofs in Dhaka and may contribute to the understanding of cool-roof impacts on local climates of tropical cities.

In this study, UHI mitigation impacts of cool roofs in Dhaka are quantitatively examined using numerical simulations for an extreme heat wave case. How the temperature reduction by cool roofs affects the air quality in Dhaka by changing boundary-layer flows and mixing is also analyzed. In section 2, simulation settings and analysis methods are provided. In section 3, diurnal variations of temperature, heat fluxes, and pollutant concentration and the impacts of cool roofs on the UHI and pollutant concentration are examined. The changes in thermal discomfort indices by cool roofs are evaluated as well. In section 4, our main findings on the cool-roof impacts on the UHI and air quality in Dhaka are summarized and future investigations needed are discussed.

## 2. Methods

To examine cool-roof impacts on the UHI and air quality in Dhaka, we conduct numerical simulations using the Weather Research and Forecasting (WRF) model version 4.1.3 (Skamarock et al., 2019). The

model set-up and physics parameterizations for this study are the same as those in Tabassum et al. (2025), being listed in Table 1. The simulation period from 0600 LST April 24, 2021 to 0600 LST April 26, 2021 is in an extreme heat wave event occurring in Bangladesh (Tabassum et al., 2025). The four one-way nested domains and the topography and land cover in the fourth domain are shown in Fig. 1. Two simulations are performed: a simulation with conventional roofs whose albedo is 0.2 (hereafter, the CONV simulation) and a simulation with cool roofs whose albedo is 0.8 (hereafter, the COOL simulation). The CONV simulation is the same as the URBAN simulation in Tabassum et al. (2025) except that the roof albedo is slightly changed from 0.12 to 0.2. The overall accuracy of 2-m temperature in the CONV simulation is similar to that in the URBAN simulation in Tabassum et al. (2025), the correlation coefficient ( $R$ ), root mean square error, and mean bias error being 0.95,  $1.72^\circ\text{C}$ , and  $-0.62^\circ\text{C}$ , respectively.

To examine cool-roof impacts on air quality, the chemistry module embedded in the WRF model (Grell et al., 2005) is activated and its passive tracer option is employed. In this option, several chemical species including carbon monoxide (CO), carbon dioxide, and methane are treated as passive tracers without chemical reactions. In this study, CO is used as a representative passive tracer to evaluate how pollutant dispersion is altered by cool roofs. A diurnally varying profile of CO emission from the surface is applied to urban grids: The daily mean emission rate is set to  $4.9 \times 10^{-7} \text{ g m}^{-2} \text{ s}^{-1}$  which corresponds to the estimated CO emissions from mobile sources in Dhaka in 2013 (Randall et al., 2015), and the diurnal variation of CO emission is based on that of the number of vehicles in Dhaka reported by Randall et al. (2015). Initial CO concentration is set to zero. Despite limitations in representing actual CO emissions in and around Dhaka, the current setup is expected to provide insights into how cool roofs influence the dispersion of air pollutants emitted from the urban areas.

To examine cool-roof impacts on human thermal comfort, four thermal discomfort indices, namely, the Humidex (Masterton and Richardson, 1979), the discomfort index (DI) (Epstein and Moran, 2006), the heat index (HI) (Rothfusz, 1990), and the wet-bulb temperature ( $T_w$ ) (Stull, 2011), in the CONV and COOL simulations are compared. The detailed calculations of these indices are presented in Kim et al. (2024). Note that the values in the urban grids are used for analysis. The analysis period is from 0600 LST April 25, 2021 to 0600 LST April 26, 2021.

## 3. Results and discussion

### 3.1. Diurnal variations of temperature and heat fluxes

The 2-m temperature and UHI intensity averaged over the urban grids in the CONV and COOL simulations are shown in Fig. 2. For calculation of UHI intensity, the urban increment method (Bohnenstengel et al., 2011) is used: The 2-m temperature averaged over the urban grids is calculated in each simulation, and then the difference

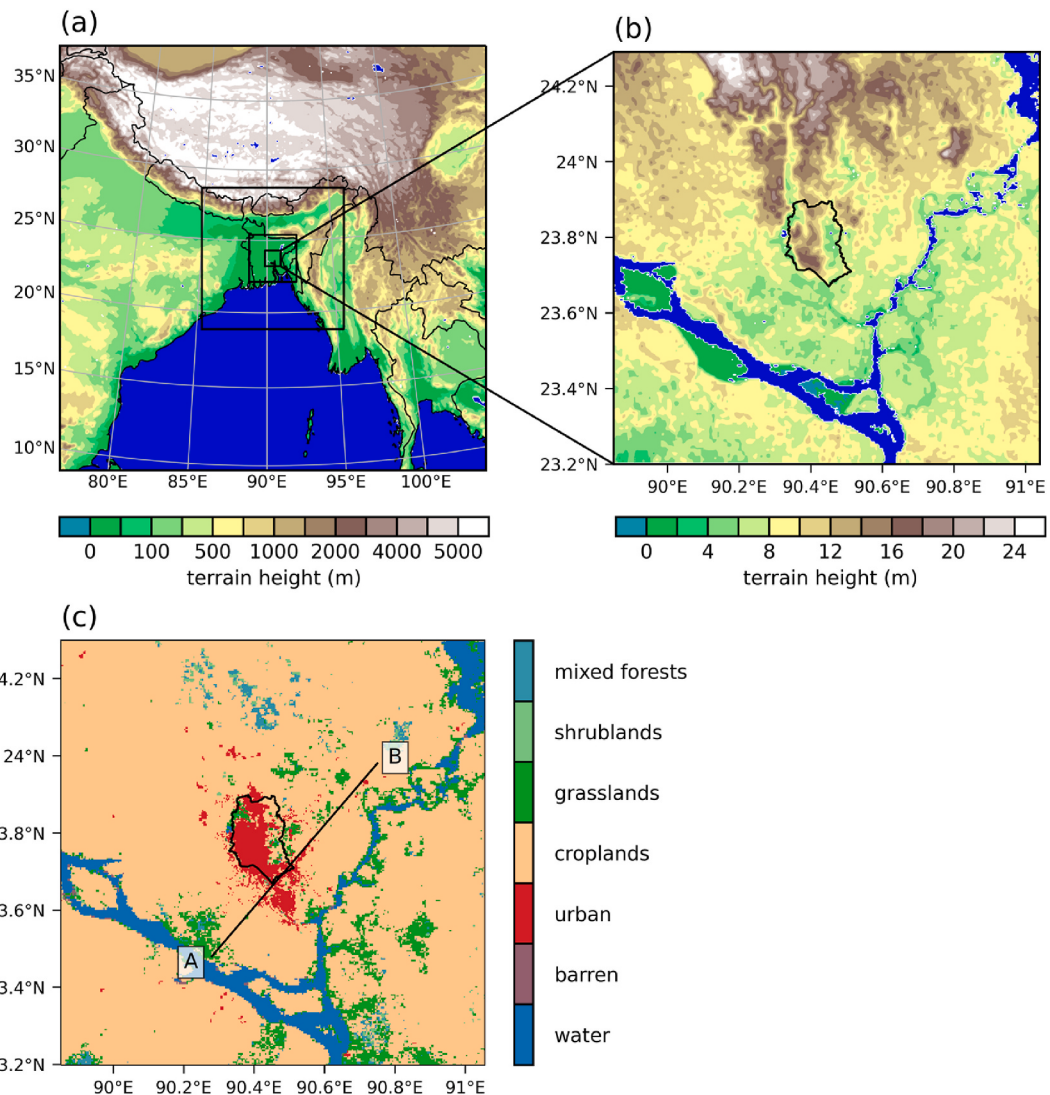


**Fig. 1.** WRF model configuration adapted from Tabassum et al. (2025). (a) Terrain height (shaded) in the four nested domains, (b) terrain height (shaded) in the fourth domain, and (c) land cover in the fourth domain. The black lines in (b) and (c) indicate the administrative boundary of Dhaka.

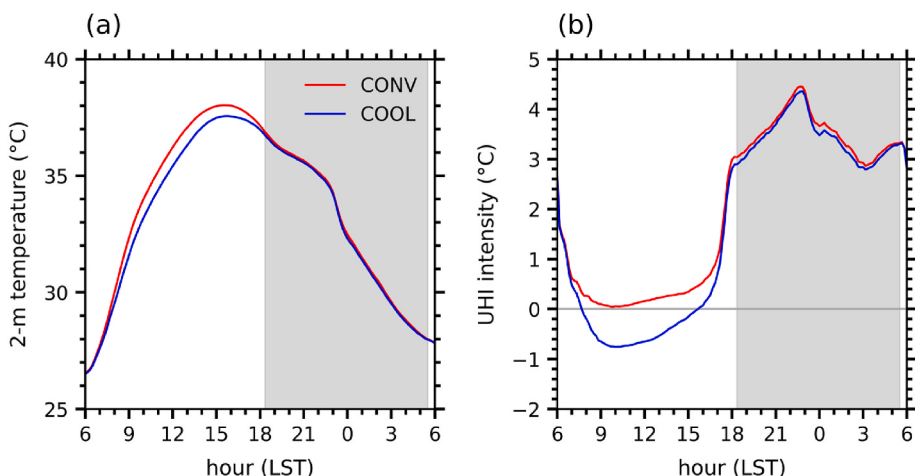


**Fig. 2.** Diurnal variations of (a) 2-m temperature and (b) UHI intensity averaged over the urban grids in the CONV (red line) and COOL (blue line) simulations. The period from sunset to sunrise is indicated by the gray shaded area.

from the 2-m temperature averaged over the corresponding grids in the simulation with urban grids being replaced by croplands (NO-URBAN simulation) is calculated. The 2-m temperature data in the NO-URBAN simulation are taken from Tabassum et al. (2025). The 2-m temperature difference between the CONV and COOL simulations (COOL minus CONV) is pronounced in the daytime (0900–1700 LST), being  $-0.65^{\circ}\text{C}$ , while it is very small in the nighttime (2100–0500 LST) (Fig. 2a). Before 0700 LST, the 2-m temperature difference between the CONV and COOL simulations is small ( $<0.10^{\circ}\text{C}$ ). The magnitude of the 2-m temperature difference increases from 0700 LST and reaches a maximum of  $0.79^{\circ}\text{C}$  at 1120 LST. The maximum 2-m temperature in the COOL simulation ( $37.6^{\circ}\text{C}$ ) is lower by  $0.4^{\circ}\text{C}$  than that in the CONV simulation ( $38.0^{\circ}\text{C}$ ).

In the CONV simulation, the UHI intensity exhibits a typical diurnal pattern with relatively low intensity in the daytime and relatively high intensity in the nighttime (Oke, 1982) (Fig. 2b). The positive UHI intensity appears throughout the day, its minimum value being  $0.04^{\circ}\text{C}$  at 0950 LST. The maximum UHI intensity is  $4.31^{\circ}\text{C}$  at 2240 LST. This peak time of UHI intensity is similar to that typically observed in Dhaka (Tabassum et al., 2024). On the other hand, in the COOL simulation, it is noticeable that the negative UHI intensity appears during 0750–1540 LST. This indicates that the urban cool island occurs in the daytime when cool roofs are installed in and around Dhaka. The mean UHI intensity in the daytime is  $0.27^{\circ}\text{C}$  in the CONV simulation and  $-0.38^{\circ}\text{C}$  in the COOL simulation. In the nighttime, the UHI intensity is still lower in the COOL simulation than in the CONV simulation but the difference in UHI intensity between the two simulations is relatively small. The mean difference in UHI intensity between the two simulations in the nighttime is  $0.10^{\circ}\text{C}$ . This slightly lower UHI intensity in the nighttime in the COOL

simulation is attributable to the reduction in the release of stored heat resulting from cool roofs, which will be discussed later.

The roof, wall, and road surface temperatures in the CONV and COOL simulations are shown in Fig. 3. The roof surface temperature in the COOL simulation is considerably lower than that in the CONV simulation throughout the day, particularly in the daytime (Fig. 3a). The heating rate of roof surface temperature during 0600–1200 LST is  $6.5^{\circ}\text{C h}^{-1}$  in the CONV simulation and  $2.6^{\circ}\text{C h}^{-1}$  in the COOL simulation, which indicates that the heating of roof surface is greatly inhibited by cool roofs. The maximum roof surface temperature in the COOL simulation ( $38.2^{\circ}\text{C}$ ) is considerably lower by  $26.4^{\circ}\text{C}$  and appears 1 h later than that in the CONV simulation ( $64.6^{\circ}\text{C}$ ). The mean roof surface temperature in the CONV (COOL) simulation in the daytime is  $58.4^{\circ}\text{C}$  ( $35.4^{\circ}\text{C}$ ). In the nighttime, the roof surface temperature is still noticeably lower in the COOL simulation than in the CONV simulation, the mean difference between the two simulations being  $5.10^{\circ}\text{C}$ . The wall (road) surface temperature overall exhibits negligible differences between the two simulations but is slightly higher in the COOL simulation than in the CONV simulation by  $1.02^{\circ}\text{C}$  ( $1.55^{\circ}\text{C}$ ) during 1320–1530 LST (1200–1710 LST) (Fig. 3b and c). Liu et al. (2024) showed that the increase in roof albedo from 0.3 to 0.7 increases road and wall surface temperatures up to  $0.46^{\circ}\text{C}$  and  $0.20^{\circ}\text{C}$ , respectively.

Cool-roof effects on urban surface energy fluxes and planetary boundary layer (PBL) height are examined. Fig. 4 shows the sensible heat flux, latent heat flux, storage heat flux, and PBL height averaged over the urban grids in the CONV and COOL simulations. In the daytime, the sensible heat flux is considerably smaller in the COOL simulation than in the CONV simulation (Fig. 4a). This is because the reflected

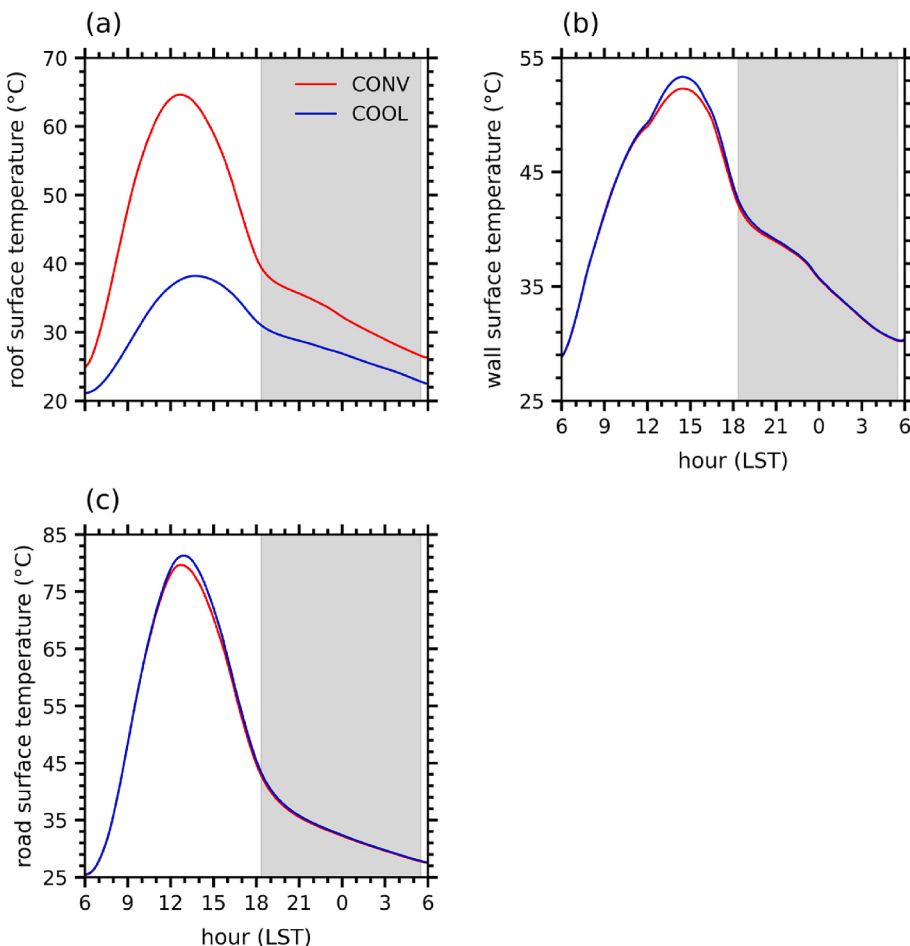


**Fig. 3.** Diurnal variations of (a) roof surface temperature, (b) wall surface temperature, and (c) road surface temperature averaged over the urban grids in the CONV (red line) and COOL (blue line) simulations. The period from sunset to sunrise is indicated by the gray shaded area.

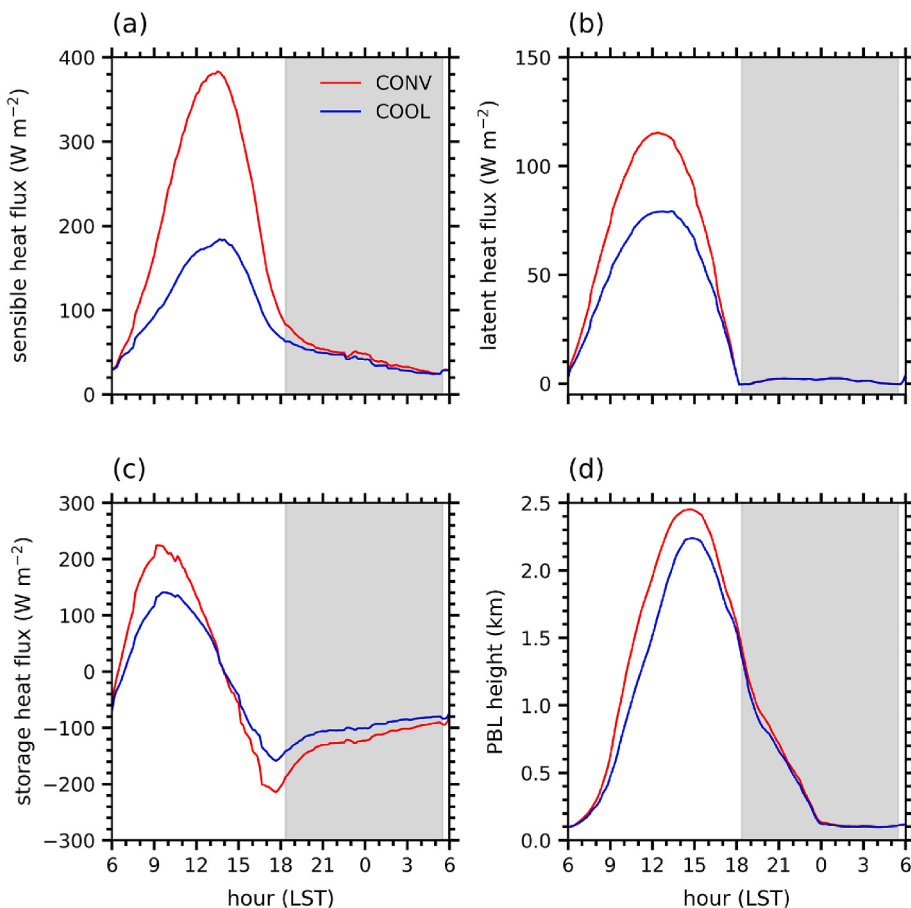


**Fig. 4.** Diurnal variations of (a) sensible heat flux, (b) latent heat flux, (c) storage heat flux, and (d) PBL height averaged over the urban grids in the CONV (red line) and COOL (blue line) simulations. The period from sunset to sunrise is indicated by the gray shaded area.

shortwave radiation at the roof surface increases due to the implementation of cool roofs. The maximum sensible heat flux in the COOL simulation ( $184 \text{ W m}^{-2}$ ) is smaller by  $199 \text{ W m}^{-2}$  than that in the CONV simulation ( $383 \text{ W m}^{-2}$ ). The mean sensible heat flux in the daytime is  $297 \text{ W m}^{-2}$  in the CONV simulation and  $146 \text{ W m}^{-2}$  in the COOL simulation. In the nighttime, the sensible heat flux is slightly lower in the COOL simulation than in the CONV simulation, the mean difference between the two simulations being  $4 \text{ W m}^{-2}$ . This marginally smaller sensible heat flux in the COOL simulation might result in the slightly lower UHI intensity in the nighttime (Fig. 2b). In the daytime, the latent heat flux is also smaller in the COOL simulation than in the CONV simulation (Fig. 4b). This results from the reduction in near-surface temperature which inhibits evapotranspiration. The maximum latent heat flux in the COOL simulation ( $79 \text{ W m}^{-2}$ ) is smaller by  $36 \text{ W m}^{-2}$  than that in the CONV simulation ( $115 \text{ W m}^{-2}$ ). The mean latent heat flux in the daytime is  $93 \text{ W m}^{-2}$  in the CONV simulation and  $65 \text{ W m}^{-2}$  in the COOL simulation. In the nighttime, the latent heat fluxes in the CONV and COOL simulations exhibit negligible differences. The noticeable decreases in sensible and latent heat fluxes resulting from the implementation of cool roofs are also found in other cities such as Seoul, South Korea (Baik et al., 2022) and Kolkata, India (Khorat et al., 2024).

As the reflected shortwave radiation at the roof surface increases due to cool roofs, the magnitude of storage heat flux is smaller in the COOL simulation than in the CONV simulation in most of the day (Fig. 4c). Compared with the CONV simulation, the heat conducted from the surface to the subsurface is reduced in the COOL simulation by  $55 \text{ W m}^{-2}$  during 0610–1330 LST and the heat conducted from the subsurface to the surface is reduced in the COOL simulation by  $23 \text{ W m}^{-2}$  during 1740–0600 LST. The smaller magnitude of nighttime storage heat flux in

the COOL simulation means less release of stored heat, leading to the marginally smaller sensible heat flux (Fig. 4a) which can result in lower UHI intensity in the nighttime (Fig. 2b).

In the daytime, the PBL height is noticeably lower in the COOL simulation than in the CONV simulation (Fig. 4d). The maximum PBL height in the COOL simulation (2250 m) is lower by 203 m than that in the CONV simulation (2453 m). The mean PBL height in the daytime is 1929 m in the CONV simulation and 1638 m in the COOL simulation. In

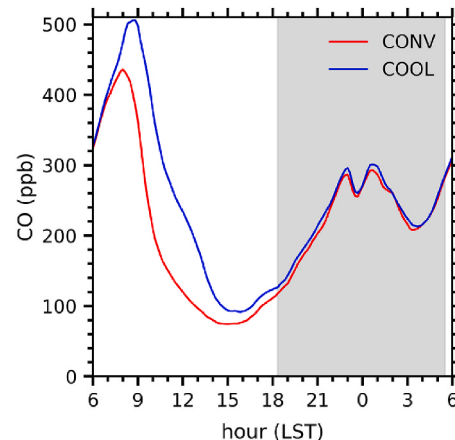


**Fig. 5.** Diurnal variations of passive tracer (CO) concentration at the lowest model level ( $z \sim 26 \text{ m}$ ) averaged over the urban grids in the CONV (red line) and COOL (blue line) simulations. The period from sunset to sunrise is indicated by the gray shaded area.

the nighttime, the PBL height in the COOL simulation is still slightly lower than that in the CONV simulation. The lower PBL height in the COOL simulation throughout the day results from the reductions in near-surface temperature (Fig. 2a) and sensible heat flux (Fig. 4a) due to cool roofs which make the PBL more stable.

In summary, the above results indicate that the city-wide implementation of cool roofs not only significantly reduces urban near-surface temperature but also considerably reduces urban turbulent and storage heat fluxes and PBL height in Dhaka in the daytime. The cool roof-induced changes in PBL characteristics in Dhaka may affect air quality. The impacts of cool roofs on air quality in Dhaka are examined in detail in the next subsection.

### 3.2. Diurnal variation of passive tracer concentration

Fig. 5 shows the passive tracer (CO) concentration at the lowest model level ( $z \sim 26$  m) averaged over the urban grids in the CONV and COOL simulations. The CO concentration in the CONV simulation clearly increases during 0600–0800 LST and peaks at 0800 LST, being 436 ppb (Fig. 5). Meanwhile, in the COOL simulation, the CO concentration peaks 50 min later than in the CONV simulation and the peak CO concentration (506 ppb) is higher by 70 ppb (16%). The rapid increases in CO concentration in the morning are attributed to very low PBL height and relatively high CO emission rate (not shown). As the PBL height increases, the CO concentration considerably decreases in both simulations. The minimum CO concentration is 74 ppb at 1500 LST in the CONV simulation and 92 ppb at 1550 LST in the COOL simulation, being 17% and 18% of the peak values in the CONV and COOL simulations, respectively. The CO concentration in the daytime is considerably higher in the COOL simulation than in the CONV simulation. The mean CO concentration in the daytime in the COOL simulation (211 ppb) is higher by 82 ppb (63%) than that in the CONV simulation (129 ppb). In the nighttime, the CO concentration is still slightly higher in the COOL simulation than in the CONV simulation, the mean difference between the two simulations being 6 ppb (2%). These results indicate that cool roofs may worsen air quality in Dhaka, particularly in the daytime.

Cool-roof impacts on the vertical distribution of passive tracer concentration are examined. Fig. 6 shows the vertical profiles of CO concentration averaged over the urban grids and over 1200–1700 LST in the CONV and COOL simulations. Hereafter, 1200–1700 LST is considered as the main analysis period and is briefly called the afternoon. In both simulations, the CO concentration monotonically decreases with

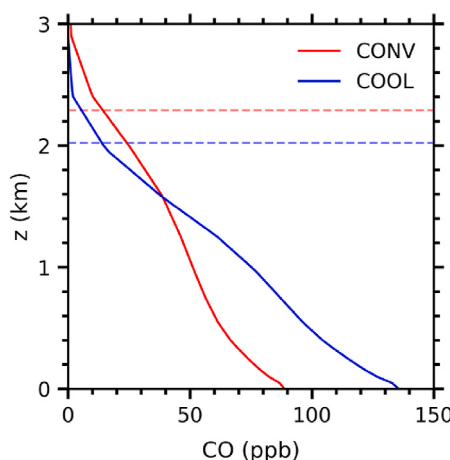


Fig. 6. Vertical profiles of CO concentration averaged over the urban grids and over 1200–1700 LST in the CONV (red solid line) and COOL (blue solid line) simulations. The red and blue dashed lines indicate the PBL heights averaged over the urban grids and over 1200–1700 LST in the CONV and COOL simulations, respectively.

increasing height. The CO concentration at the lowest model level (PBL top height) is 87 ppb (14 ppb) in the CONV simulation and 132 ppb (14 ppb) in the COOL simulation. The decrease in CO concentration with increasing height, in spite of the development of the mixed layer in the afternoon, is due to the absence of initial background concentrations in both simulations. In an additional simulation where the initial CO concentration is uniformly set to 87 ppb, which is the mean lowest model level CO concentration in the CONV simulation, the CO concentration is nearly uniform within the mixed layer in the afternoon (not shown). Below  $z \sim 1.6$  km, the CO concentration in the COOL simulation is noticeably higher than that in the CONV simulation, the mean difference between the two simulations being 26 ppb. Meanwhile, above  $z \sim 1.6$  km, the CO concentration in the COOL simulation is lower than that in the CONV simulation, the mean difference between the two simulations being 2 ppb. These are attributed to the weaker vertical mixing within the PBL in the COOL simulation. The mean PBL height in the afternoon in the COOL simulation (2015 m) is lower by 265 m than that in the CONV simulation (2280 m). These results indicate that the cool roof-induced reduction in vertical turbulent mixing within the PBL is closely associated with the increase in near-surface CO concentration in and around Dhaka, which will be further investigated in the next subsection.

### 3.3. Impacts of cool roofs on the UHI and passive tracer concentration

In this subsection, cool-roof impacts on the UHI and passive tracer concentration are further analyzed in detail. Fig. 7 shows the fields of 2-m temperature, 10-m horizontal wind vector, and CO concentration averaged over the afternoon in the CONV and COOL simulations and their respective differences (COOL minus CONV). In Dhaka and its surrounding rural areas, an anticyclonic pattern is prevalent with low wind speed ( $<2.0 \text{ m s}^{-1}$ ) due to a high-pressure system located southwest of Bangladesh (Tabassum et al., 2025). In the CONV simulation, the 2-m temperature is overall higher in the urban areas, especially in the central region and southeast of Dhaka with a maximum of  $38.0^\circ\text{C}$  (Fig. 7a). In contrast, in the COOL simulation, the 2-m temperature in the urban areas is similar to or slightly lower than the 2-m temperature in their nearby areas (Fig. 7b). In addition, the 10-m wind speed averaged over the urban areas is lower by  $0.8 \text{ m s}^{-1}$  in the COOL simulation than that in the CONV simulation. The differences in 2-m temperature and 10-m horizontal wind between the CONV and COOL simulations (COOL minus CONV) are seen in Fig. 7c. The clear negative difference in 2-m temperature is found in the urban areas and their nearby areas. The difference is particularly pronounced in the central region and southeast of Dhaka where the 2-m temperature in the CONV simulation is relatively high. This means that cool roofs tend to reduce near-surface temperature more in hotter areas. The maximum magnitude of the negative difference in 2-m temperature is  $1.02^\circ\text{C}$  and appears in the southeast of Dhaka ( $23.71^\circ\text{N}, 90.51^\circ\text{E}$ ). The wind difference is overall diverging from the downwind of Dhaka. This is due to the suppression of the urban breeze that is induced by the UHI (Hidalgo et al., 2008) and blows toward the downwind of Dhaka near the surface. The wind difference in the urban areas is opposite to the prevailing winds, its mean magnitude being  $0.9 \text{ m s}^{-1}$ . This indicates that the suppression of the UHI due to cool roofs could reduce the wind speed in and around Dhaka.

The CO concentration in the CONV simulation is also higher in the central region and southeast of Dhaka, with a maximum concentration of 183 ppb (Fig. 7d). CO is advected along the prevailing winds, mainly toward the east of Dhaka. In the COOL simulation, the CO concentration is noticeably higher than that in the CONV simulation, especially being high in the central-northern region and southeast of Dhaka (Fig. 7e). This is associated with the reductions in PBL height and near-surface wind speed due to cool roofs (Figs. 6 and 7b). The maximum CO concentration is 256 ppb and appears in the central-northern region of Dhaka. The difference in CO concentration between the CONV and COOL simulations (COOL minus CONV) is seen in Fig. 7f. Overall, the

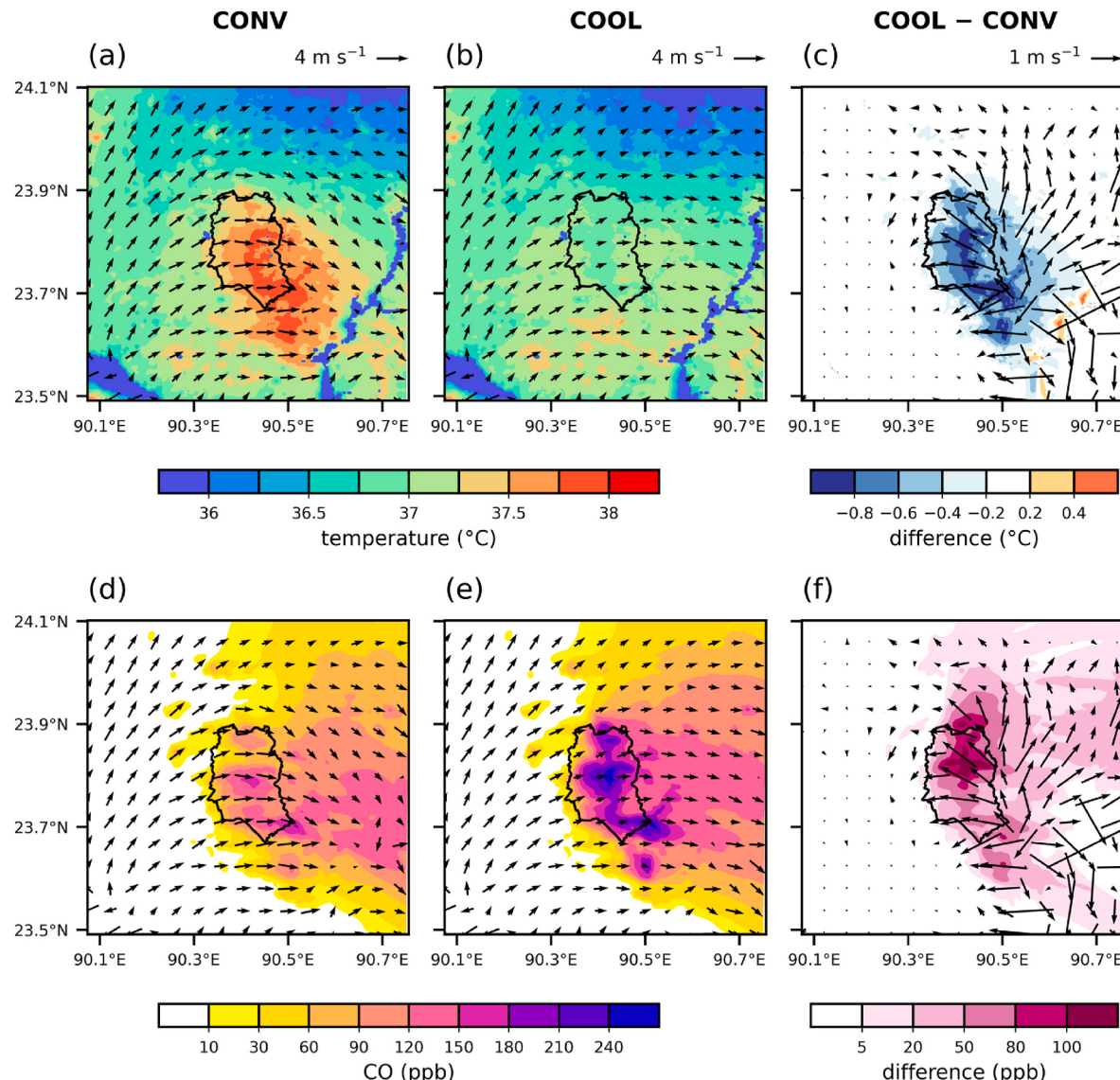


**Fig. 7.** Fields of 2-m temperature (shaded) and 10-m horizontal wind vector (arrows) averaged over 1200–1700 LST in the (a) CONV and (b) COOL simulations and (c) their respective differences (COOL minus CONV). Fields of CO concentration at the lowest model level ( $z \sim 26$  m) (shaded) and 10-m horizontal wind vector (arrows) averaged over 1200–1700 LST in the (d) CONV and (e) COOL simulations and (f) their respective differences (COOL minus CONV). The black line indicates the administrative boundary of Dhaka.

positive difference in CO concentration is found. The difference is particularly large in the central-northern region of Dhaka, its maximum value being 124 ppb (Fig. 7f). Henao et al. (2020) and Park and Baik (2024), which treat passive tracers in a similar way to this study, also found substantial increases in tracer concentration resulting from UHI mitigation measures. Interestingly, the difference in CO concentration tends to be pronounced in the region where the difference in 2-m temperature is large,  $R$  between them being  $-0.78$  and statistically significant at  $p < 0.01$  (Fig. 7c and f). This is because the cool roof-induced reductions in PBL height and 10-m wind speed tend to be larger in the region where the cool roof-induced reduction in 2-m temperature is large.  $R$  between the difference in PBL height (10-m wind speed) between the two simulations and the difference in 2-m temperature between the two simulations is  $0.92$  ( $0.71$ ) and is statistically significant at  $p < 0.01$ . Meanwhile,  $R$  between the difference in PBL height (10-m wind speed) between the two simulations and the difference in CO concentration between the two simulations is  $-0.62$  ( $-0.61$ ) and is statistically significant at  $p < 0.01$ . This result indicates that both cool roof-induced reduction in PBL height and that in near-surface wind

speed are important contributors to the cool roof-induced increase in CO concentration.

Zhang et al. (2019) showed that the variability of the increase in primary pollutants due to cool roofs in Southern California is better explained by the reduction in wind speed than the reduction in PBL height. To further examine the relative importance of the difference in PBL height between the two simulations and the difference in 10-m wind speed between the two simulations to the difference in CO concentration, a multiple linear regression analysis is conducted. The analysis reveals that the differences in PBL height and 10-m wind speed explain 50 % of the total variance of the difference in CO concentration. The standardized regression coefficients of the difference in PBL height and the difference in 10-m wind speed are, respectively,  $-0.42$  and  $-0.40$ , and these coefficients are statistically significant at  $p < 0.01$ . This indicates that the differences in PBL height and 10-m wind speed are comparably important.

The vertical cross sections of the differences in potential temperature, horizontal wind, and passive tracer concentration between the CONV and COOL simulations (COOL minus CONV) averaged over the

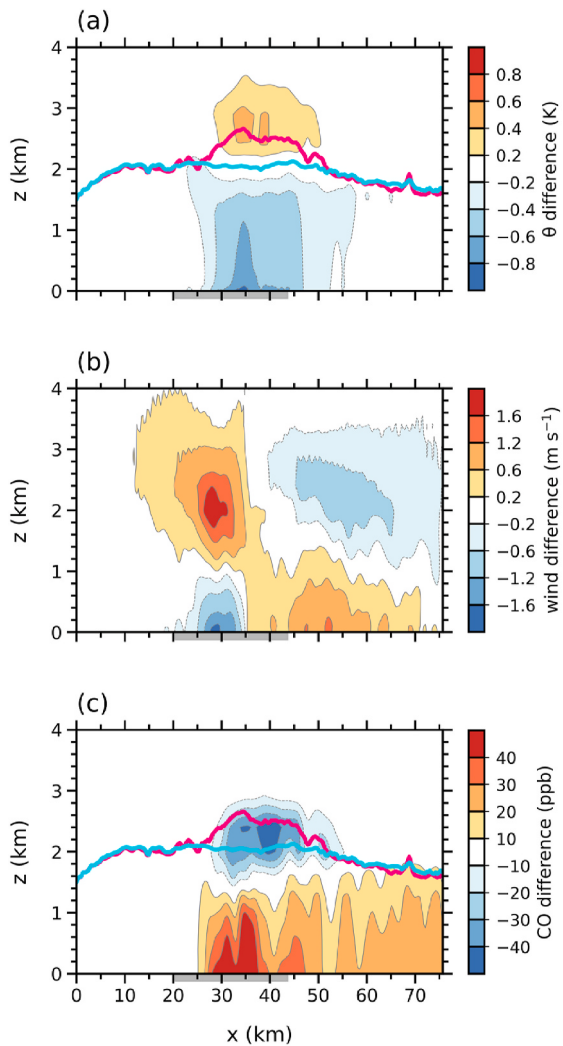


**Fig. 8.** Vertical cross sections of the differences in (a) potential temperature, (b) horizontal wind, and (c) CO concentration between the CONV and COOL simulations (COOL minus CONV) averaged over 1200–1700 LST along the line A–B (see Fig. 1c). The pink (blue) lines in (a) and (c) indicate the PBL height averaged over 1200–1700 LST in the CONV (COOL) simulation. The gray box on the x-axis indicates the major urban areas along the line A–B.

afternoon along the line A–B (Fig. 1c) are shown in Fig. 8. The line A–B is adopted because the cool-roof effects on the urban breeze circulation (UBC) are well represented along the line A–B. The major urban area is situated over  $x \sim 20$ –44 km along the line A–B. The cool roof-induced reduction in potential temperature is found throughout the PBL and is most pronounced ( $-0.89$  K) at  $x \sim 34$  km (Fig. 8a). The mean difference in potential temperature between the two simulations over  $z \sim 0.0$ –1.5 km in the major urban area is  $-0.41$  K. The reduction in PBL height due to cool roofs appears over the major urban area and its just nearby area, while being negligible far outside the major urban area. The wind difference which is opposed to the UBC is pronounced along the line A–B, indicating that the UBC is strongly suppressed due to cool roofs (Fig. 8b). The maximum horizontal wind difference is  $1.9$  m  $s^{-1}$  and appears near the PBL top height ( $z \sim 2.0$  km) in the major urban area. The increase in CO concentration due to cool roofs appears over  $z \sim 0.0$ –1.5 km and is most pronounced (68 ppb) at  $x \sim 35$  km (Fig. 8c). The mean difference in CO concentration between the two simulations over  $z \sim 0.0$ –1.5 km in the major urban area is 20 ppb. The positive difference in CO

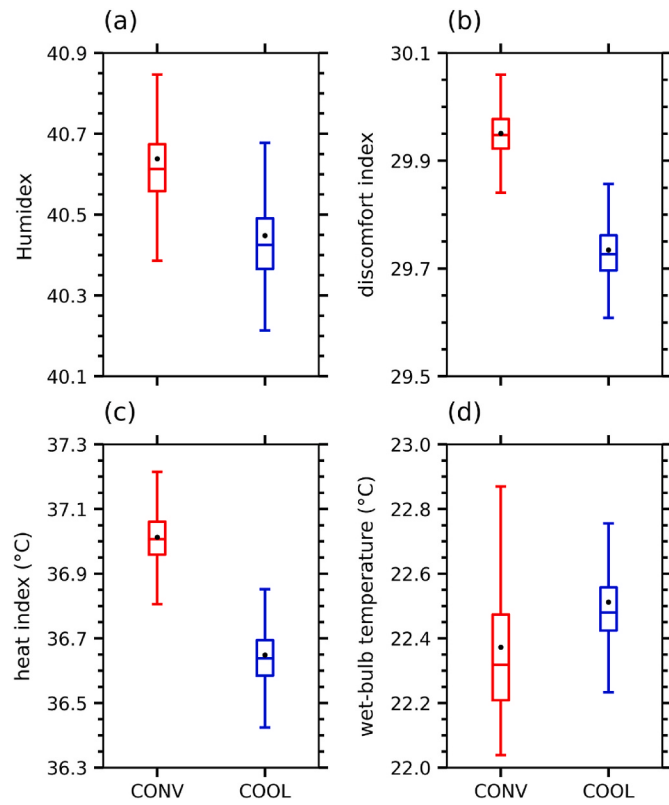


**Fig. 9.** Box plots of (a) Humidex, (b) discomfort index, (c) heat index, and (d) wet-bulb temperature averaged over 1200–1700 LST in the urban grids in the CONV and COOL simulations. The black dot and horizontal line in each box indicate the mean and median, respectively. The upper and lower edges of each box indicate the upper and lower quartiles, respectively. The whiskers above and below each box indicate the 90th and 10th percentiles, respectively.

concentration between the two simulations also appears over  $x \sim 45$ –75 km. This is because the transport of CO from the major urban area increases due to both the increase in CO concentration in the major urban area and changes in wind direction which result from cool roofs (Fig. 7f).

### 3.4. Cool-roof effects on urban heat stress

In this subsection, cool-roof effects on urban heat stress in and around Dhaka are analyzed. Fig. 9 shows the box plots of the four thermal discomfort indices (Humidex, DI, HI, and  $T_w$ ) averaged over the afternoon in the urban grids in the CONV and COOL simulations. In the afternoon, the mean 2-m temperature is lower by  $0.57$  °C in the COOL simulation than in the CONV simulation while the mean relative humidity and water vapor mixing ratio are higher by 1.90 %p and  $0.43$  g  $kg^{-1}$  in the COOL simulation. The higher water vapor mixing ratio in the COOL simulation, despite the smaller latent heat flux in the COOL simulation than in the CONV simulation, is attributed to the cool-roof induced reduction in vertical mixing. In the CONV simulation, Humidex is in the “great discomfort” level ( $40 \leq \text{Humidex} \leq 45$ ) (Blazejczyk et al., 2012), DI is in the level in which “everyone feels severe stress” ( $29 \leq \text{DI} < 32$ ) (Poupouk et al., 2011), and HI is in the “extreme caution” level ( $32 \leq \text{HI} < 41$ ) (Blazejczyk et al., 2012) in the afternoon.  $T_w$  in the afternoon is not in the “intolerable” level ( $T_w > 35$  °C) (Sherwood and Huber, 2010).

Compared with the CONV simulation, the statistical distributions of Humidex, DI, and HI in the COOL simulation exhibit decreasing shifts

which are statistically significant at  $p < 0.01$  (Fig. 9a–c). The mean Humidex, DI, and HI are, respectively, lower by 0.19, 0.22, and 0.36 °C in the COOL simulation than in the CONV simulation. These reductions in Humidex, DI, and HI are attributed to the cool roof-induced reduction in 2-m temperature. The interquartile ranges (upper quartile minus lower quartile) of Humidex, DI, and HI are, respectively, 0.11, 0.06, and 0.10 °C in the CONV simulation and these hardly change in the COOL simulation. This means that cool roofs do not significantly change the spatial variabilities of Humidex, DI, and HI in and around Dhaka. On the other hand, compared with the CONV simulation, the statistical distribution of  $T_w$  exhibits an increasing shift which is statistically significant at  $p < 0.01$  (Fig. 9d). The mean  $T_w$  in the COOL simulation is higher by 0.14 °C than that in the CONV simulation. This is attributed to the cool roof-induced increase in relative humidity. Kim et al. (2024) showed that the sensitivity of  $T_w$  to relative humidity is larger than those of Humidex, DI, and HI. Thus, since the relative importance of temperature and humidity to each thermal discomfort index is different, the effects of cool roofs on urban heat stress may be differently interpreted depending on the choice of thermal discomfort index. The interquartile range of  $T_w$  in the CONV (COOL) simulation is 0.26 (0.14) °C, meaning that the spatial variability of  $T_w$  in and around Dhaka is reduced when the implementation of cool roofs is conducted. Despite the statistically significant decreases in Humidex, DI, and HI due to cool roofs, Humidex, DI, and HI in the COOL simulation are still in the same stress levels as those in the CONV simulation. This indicates that cool roofs alone may not be an effective solution to mitigate urban heat stress during heat waves in and around Dhaka, which requires additional measures such as urban greenery and other climate-sensitive urban designs and plannings.

#### 4. Summary and conclusions

Rapid urbanization has brought about thermal discomfort as well as air pollution in Dhaka. Despite the issues, the UHI mitigation effect of cool roofs and the accompanied changes in air quality in Dhaka have not been examined yet in detail. In this study, we investigate cool-roof impacts on the UHI and air quality in Dhaka during an extreme heat wave event using the WRF model. A simulation with conventional roofs whose albedo is 0.2 (CONV) and a simulation with cool roofs whose albedo is 0.8 (COOL) are conducted and compared. In the afternoon, cool roofs reduce the 2-m temperature by 0.57 °C, playing a role in mitigating urban heat stress as in other cities (e.g., Santamouris, 2014). Meanwhile, cool roofs increase the near-surface passive tracer (CO) concentration by 45 ppb (52 %) as they reduce PBL height and near-surface wind speed. This implies the necessity for careful preliminary survey of unintended worsening of air quality before a practical application of cool roofs. Changes in near-surface temperature, wind speed, and CO concentration and PBL height due to cool roofs are overall larger in hotter areas. The implementation of cool roofs causes statistically significant differences in thermal discomfort indices, but all indices remain within the same stress levels. This suggests that the application of additional measures together with cool roofs is needed for more effective mitigation of urban extreme heat in and around Dhaka. The quantitative results for the CONV and COOL simulations and their differences are summarized in Table 2.

In this study, a passive tracer is used to investigate cool-roof impacts on air quality in Dhaka. Since there exist many air pollutants and their emission rates and temporal/spatial distributions are different, cool-roof impacts on their concentrations can significantly differ depending on air pollutants. Furthermore, the concentrations of secondary air pollutants such as ozone and fine particulate matters may vary in complex ways due to cool roofs because changes in both temperature and wind affect their chemical reactions. To better understand cool-roof impacts on

**Table 2**

Values of key variables averaged over the urban grids and over 1200–1700 LST in the CONV and COOL simulations and their differences.

	CONV	COOL	COOL–CONV
2-m temperature (°C)	37.5	37.0	-0.57
PBL height (m)	2280	2015	-265
10-m wind speed (m s <sup>-1</sup> )	2.4	1.5	-0.8
Near-surface CO concentration (ppb)	87	132	45
Humidex	40.64	40.45	-0.19
DI	29.95	29.73	-0.22
HI (°C)	37.0	36.7	-0.36
$T_w$ (°C)	22.4	22.5	0.14

various air pollutants in Dhaka, further studies using a numerical model coupled with a full-chemistry model (e.g., Grell et al., 2005; Byun and Schere, 2006) and high-resolution emission inventories are needed. Turbulent structures within the PBL greatly affect the dispersion of air pollutants (Han et al., 2019), and their changes due to cool roofs modify air quality in complex ways (Han et al., 2020). However, cool roof-induced changes in turbulent structures and their impacts on air quality in Dhaka are difficult to be examined in our current simulations with a PBL parameterization. Further investigations of cool-roof impacts using high-resolution large-eddy simulations will be helpful to examine these aspects. It has been recently reported that combining different mitigation measures works more effectively than implementing only one mitigation measure (Chatterjee et al., 2019; Zhang and Hu, 2024). To find an optimal way to effectively mitigate urban heat stress in Dhaka, various mitigation measures and their combined effects need to be investigated.

#### CRediT authorship contribution statement

**Abeda Tabassum:** Writing – original draft, Visualization, Validation, Investigation, Formal analysis, Data curation. **Kyeongjoo Park:** Writing – review & editing, Investigation, Formal analysis. **Seong-Ho Hong:** Writing – review & editing, Investigation, Formal analysis. **Jong-Jin Baik:** Writing – review & editing, Supervision, Conceptualization. **Beom-Soon Han:** Writing – review & editing, Investigation.

#### Declaration of competing interest

The authors declare that they have no known competing financial interests or personal relationships that could have appeared to influence the work reported in this paper.

#### Acknowledgements

The authors are grateful to two anonymous reviewers for providing valuable comments on this work. This work was supported by the National Research Foundation of Korea (NRF) under grant RS-2025-00562044.

#### References

- Abrar, R., Sarkar, S.K., Nishtha, K.T., Talukdar, S., Shahfahad, Rahman, A., Islam, A.R.M. T., Mosavi, A., 2022. Assessing the spatial mapping of heat vulnerability under urban heat island (UHI) effect in the Dhaka metropolitan area. *Sustainability* 14, 4945.
- Akbari, H., Pomerantz, M., Taha, H., 2001. Cool surfaces and shade trees to reduce energy use and improve air quality in urban areas. *Sol. Energy* 70, 295–310.
- Bach, A.J.E., Palutikof, J.P., Tonmoy, F.N., Smallcombe, J.W., Rutherford, S., Joarder, A. R., Hossain, M., Jay, O., 2023. Retrofitting passive cooling strategies to combat heat stress in the face of climate change: a case study of a ready-made garment factory in Dhaka, Bangladesh. *Energy Build.* 286, 112954.
- Baik, J.-J., Lim, H., Han, B.-S., Jin, H.-G., 2022. Cool-roof effects on thermal and wind environments during heat waves: a case modeling study in Seoul, South Korea. *Urban Clim.* 41, 101044.

- Baniassadi, A., Sailor, D.J., Ban-Weiss, G.A., 2019. Potential energy and climate benefits of super-cool materials as a rooftop strategy. *Urban Clim.* 29, 100495.
- BBS, 2022. Population and Housing Census 2022: Preliminary Report. Bangladesh Bureau of Statistics, Dhaka, p. 55.
- Beck, H.E., Zimmermann, N.E., McVicar, T.R., Vergoplán, N., Berg, A., Wood, E.F., 2018. Present and future Köppen-Geiger climate classification maps at 1-km resolution. *Sci. Data* 5, 180214.
- Blazejczyk, K., Epstein, Y., Jendritzky, G., Staiger, H., Tinz, B., 2012. Comparison of UTCI to selected thermal indices. *Int. J. Biometeorol.* 56, 515–535.
- Bohnenstengel, S.I., Evans, S., Clark, P.A., Belcher, S.E., 2011. Simulations of the London urban heat island. *Q. J. R. Meteorol. Soc.* 137, 1625–1640.
- Byun, D., Schere, K.L., 2006. Review of the governing equations, computational algorithms, and other components of the Models-3 Community Multiscale Air Quality (CMAQ) modeling system. *Appl. Mech. Rev.* 59, 51–77.
- Cao, M., Rosado, P., Lin, Z., Levinson, R., Millstein, D., 2015. Cool roofs in Guangzhou, China: outdoor air temperature reductions during heat waves and typical summer conditions. *Environ. Sci. Technol.* 49, 14672–14679.
- Chatterjee, S., Khan, A., Dinda, A., Mithun, S., Khatun, R., Akbari, H., Kusaka, H., Mitra, C., Bhatti, S.S., Doan, Q.V., Wang, Y., 2019. Simulating micro-scale thermal interactions in different building environments for mitigating urban heat islands. *Sci. Total Environ.* 663, 610–631.
- Chen, F., Dudhia, J., 2001. Coupling an advanced land surface-hydrology model with the Penn State-NCAR MM5 modeling system. Part I: model implementation and sensitivity. *Mon. Weather Rev.* 129, 569–585.
- Dudhia, J., 1989. Numerical study of convection observed during the Winter Monsoon Experiment using a mesoscale two-dimensional model. *J. Atmos. Sci.* 46, 3077–3107.
- Elnabawi, M.H., Hamza, N., Raveendran, R., 2023. ‘Super cool roofs’: mitigating the UHI effect and enhancing urban thermal comfort with high albedo-coated roofs. *Results Eng.* 19, 101269.
- Epstein, S.A., Lee, S.-M., Katzenstein, A.S., Carreras-Sospedra, M., Zhang, X., Farina, S.C., Vahmani, P., Fine, P.M., Ban-Weiss, G., 2017. Air-quality implications of widespread adoption of cool roofs on ozone and particulate matter in southern California. *Proc. Natl. Acad. Sci. U.S.A.* 114, 8991–8996.
- Epstein, Y., Moran, D.S., 2006. Thermal comfort and the heat stress indices. *Ind. Health* 44, 388–398.
- Falasca, S., Curci, G., 2018. Impact of highly reflective materials on meteorology, PM10 and ozone in urban areas: a modeling study with WRF-CHIMERE at high resolution over Milan (Italy). *Urban Sci.* 2, 18.
- Fallmann, J., Forkel, R., Emeis, S., 2016. Secondary effects of urban heat island mitigation measures on air quality. *Atmos. Environ.* 125, 199–211.
- Grell, G.A., Peckham, S.E., Schmitz, R., McKeen, S.A., Frost, G., Skamarock, W.C., Eder, B., 2005. Fully coupled “online” chemistry within the WRF model. *Atmos. Environ.* 39, 6957–6975.
- Han, B.-S., Baik, J.-J., Kwak, K.-H., 2019. A preliminary study of turbulent coherent structures and ozone air quality in Seoul using the WRF-CMAQ model at a 50 m grid spacing. *Atmos. Environ.* 218, 117012.
- Han, B.-S., Baik, J.-J., Kwak, K.-H., Park, S.-B., 2020. Effects of cool roofs on turbulent coherent structures and ozone air quality in Seoul. *Atmos. Environ.* 229, 117476.
- He, C., Zhao, J., Zhang, Y., He, L., Yao, Y., Ma, W., Kinney, P.L., 2020. Cool roof and green roof adoption in a metropolitan area: climate impacts during summer and winter. *Environ. Sci. Technol.* 54, 10831–10839.
- Henaq, J.J., Rendón, A.M., Salazar, J.F., 2020. Trade-off between urban heat island mitigation and air quality in urban valleys. *Urban Clim.* 31, 100542.
- Hersbach, H., Bell, B., Berrisford, P., Hirahara, S., Horányi, A., Muñoz-Sabater, J., Nicolas, J., Peubey, C., Radu, R., Schepers, D., Simmons, A., Soci, C., Abdalla, S., Abellán, X., Balsamo, G., Bechtold, P., Biavati, G., Bidlot, J., Bonavita, M., Chiara, G., Dahlgren, P., Dee, D., Diamantakis, M., Dragani, R., Flemming, J., Forbes, R., Fuentes, M., Geer, A., Haimes, L., Healy, S., Hogan, R.J., Holm, E., Janisková, M., Keeley, S., Laloyaux, P., Lopez, P., Lupu, C., Radnoti, G., de Rosnay, P., Rozum, I., Vamborg, F., Villaume, S., Thépaut, J.-N., 2020. The ERA5 global reanalysis. *Q. J. R. Meteorol. Soc.* 146, 1999–2049.
- Hidalgo, J., Masson, V., Pigeon, G., 2008. Urban-breeze circulation during the CAPITOUL experiment: numerical simulations. *Meteorol. Atmos. Phys.* 102, 243–262.
- Ho, J.Y., Shi, Y., Lau, K.K.L., Ng, E.Y.Y., Ren, C., Goggins, W.B., 2023. Urban heat island effect-related mortality under extreme heat and non-extreme heat scenarios: a 2010–2019 case study in Hong Kong. *Sci. Total Environ.* 858, 159791.
- Hong, S.-Y., Noh, Y., Dudhia, J., 2006. A new vertical diffusion package with an explicit treatment of entrainment processes. *Mon. Weather Rev.* 134, 2318–2341.
- Imran, H.M., Hossain, A., Islam, A.K.M.S., Rahman, A., Bhuiyan, M.A.E., Paul, S., Alam, A., 2021. Impact of land cover changes on land surface temperature and human thermal comfort in Dhaka city of Bangladesh. *Earth Syst. Environ.* 5, 667–693.
- Imran, H.M., Kala, J., Ng, A.W.M., Muthukumaran, S., 2018. Effectiveness of green and cool roofs in mitigating urban heat island effects during a heatwave event in the city of Melbourne in southeast Australia. *J. Clean. Prod.* 197, 393–405.
- Jandaghian, Z., Akbari, H., 2018. The effect of increasing surface albedo on urban climate and air quality: a detailed study for Sacramento, Houston, and Chicago. *Climate* 6, 19.
- Jiménez, P.A., Dudhia, J., González-Rouco, J.F., Navarro, J., Montávez, J.P., García-Bustamante, E., 2012. A revised scheme for the WRF surface layer formulation. *Mon. Weather Rev.* 140, 898–918.
- Kain, J.S., 2004. The Kain-Fritsch convective parameterization: an update. *J. Appl. Meteorol.* 43, 170–181.
- Khorat, S., Das, D., Khatun, R., Aziz, S.M., Anand, P., Khan, A., Santamouris, M., Niyyogi, D., 2024. Cool roof strategies for urban thermal resilience to extreme heatwaves in tropical cities. *Energy Build.* 302, 113751.
- Kim, D.-H., Park, K., Baik, J.-J., Jin, H.-G., Han, B.-S., 2024. Contrasting interactions of urban heat islands with dry and moist heat waves and their implications for urban heat stress. *Urban Clim.* 56, 102050.
- Lai, L.-W., Cheng, W.-L., 2009. Air quality influenced by urban heat island coupled with synoptic weather patterns. *Sci. Total Environ.* 407, 2724–2733.
- Li, D., Bou-Zeid, E., 2013. Synergistic interactions between urban heat islands and heat waves: the impact in cities is larger than the sum of its parts. *J. Appl. Meteorol. Climatol.* 52, 2051–2064.
- Li, X.-X., Norford, L.K., 2016. Evaluation of cool roof and vegetations in mitigating urban heat island in a tropical city, Singapore. *Urban Clim.* 16, 59–74.
- Lim, K.-S.S., Hong, S.-Y., 2010. Development of an effective double-moment cloud microphysics scheme with prognostic cloud condensation nuclei (CCN) for weather and climate models. *Mon. Weather Rev.* 138, 1587–1612.
- Liu, Y., Chu, C., Zhang, R., Chen, S., Xu, C., Zhao, D., Meng, C., Ju, M., Cao, Z., 2024. Impacts of high-albedo urban surfaces on outdoor thermal environment across morphological contexts: a case of Tianjin, China. *Sust. Cities Soc.* 100, 105038.
- Macintyre, H.L., Heaviside, C., 2019. Potential benefits of cool roofs in reducing heat-related mortality during heatwaves in a European city. *Environ. Int.* 127, 430–441.
- Masterton, J.M., Richardson, F.A., 1979. Humidex: a Method of Quantifying Human Discomfort due to Excessive Heat and Humidity. Environment Canada, Atmospheric Environment, Downsview, p. 45.
- Mlawer, E.J., Taubman, S.J., Brown, P.D., Iacono, M.J., Clough, S.A., 1997. Radiative transfer for inhomogeneous atmospheres: RRTM, a validated correlated-k model for the longwave. *J. Geophys. Res. Atmos.* 102, 16663–16682.
- Nissan, H., Burkart, K., de Perez, E.C., Van Aalst, M., Mason, S., 2017. Defining and predicting heat waves in Bangladesh. *J. Appl. Meteorol. Climatol.* 56, 2653–2670.
- Oke, T.R., 1982. The energetic basis of the urban heat island. *Q. J. R. Meteorol. Soc.* 108, 1–24.
- Park, K., Baik, J.-J., 2024. Nonlinear changes in urban heat island intensity, urban breeze intensity, and urban air pollutant concentration with roof albedo. *Sci. Rep.* 14, 24911.
- Phelan, P.E., Kaloush, K., Miner, M., Golden, J., Phelan, B., Silva III, H., Taylor, R.A., 2015. Urban heat island: mechanisms, implications, and possible remedies. *Annu. Rev. Environ. Resour.* 40, 285–307.
- Poupoukou, A., Nastos, P., Melas, D., Zerefos, C., 2011. Climatology of discomfort index and air quality index in a large urban Mediterranean agglomeration. *Water Air Soil Pollut.* 222, 163–183.
- Rahman, M.M., Mahamud, S., Thurston, G.D., 2019. Recent spatial gradients and time trends in Dhaka, Bangladesh, air pollution and their human health implications. *J. Air Waste Manag. Assoc.* 69, 478–501.
- Randall, S., Sivertsen, B., Ahammad, S.S., Cruz, N.D., Dam, V.T., 2015. Emissions Inventory for Dhaka and Chittagong of Pollutants PM<sub>10</sub>, PM<sub>2.5</sub>, NO<sub>x</sub>, SO<sub>x</sub>, and CO. NILU OR 45/2014, Norwegian Institute for Air Research, Kjeller, p. 96.
- Rawat, M., Singh, R.N., 2022. A study on the comparative review of cool roof thermal performance in various regions. *Energy Built Environ.* 3, 327–347.
- Rawat, M., Singh, D., Buddhi, D., 2022. Thermal performance of cool roofs incorporated with phase change materials: a review. *Mater. Today Proc.* 69, 392–400.
- Razzaghmanesh, M., Beecham, S., Salemi, T., 2016. The role of green roofs in mitigating urban heat island effects in the metropolitan area of Adelaide, South Australia. *Urban For. Urban Green.* 15, 89–102.
- Reed, K., Sun, F., 2023. Investigating the potential for cool roofs to mitigate urban heat in the Kansas City metropolitan area. *Clim. Dyn.* 60, 461–475.
- Roman, K.K., O’Brien, T., Alvey, J.B., Woo, O., 2016. Simulating the effects of cool roof and PCM (phase change materials) based roof to mitigate UHI (urban heat island) in prominent US cities. *Energy* 96, 103–117.
- Rothfuss, L.P., 1990. The Heat Index “Equation” (or, More than You Ever Wanted to Know About Heat Index). SR 90-23, National Weather Service, Fort Worth, p. 2.
- Ryu, Y.-H., Baik, J.-J., Lee, S.-H., 2011. A new single-layer urban canopy model for use in mesoscale atmospheric models. *J. Appl. Meteorol. Climatol.* 50, 1773–1794.
- Santamouris, M., 2014. Cooling the cities – a review of reflective and green roof mitigation technologies to fight heat island and improve comfort in urban environments. *Sol. Energy* 103, 682–703.
- Santamouris, M., Cartalis, C., Synnefa, A., Kolokotsa, D., 2015. On the impact of urban heat island and global warming on the power demand and electricity consumption of buildings—a review. *Energy Build.* 98, 119–124.
- Sherwood, S.C., Huber, M., 2010. An adaptability limit to climate change due to heat stress. *Proc. Natl. Acad. Sci. U.S.A.* 107, 9552–9555.
- Skamarock, W.C., Klemp, J.B., Dudhia, J., Gill, D.O., Liu, Z., Berner, J., Wang, W., Powers, J.G., Duda, M.G., Barker, D.M., Huang, X.-Y., 2019. A Description of the Advanced Research WRF Model Version 4. NCAR Tech. Note TN-556+STR. National Center for Atmospheric Research, Boulder, p. 148 pp.
- Stull, R., 2011. Wet-bulb temperature from relative humidity and air temperature. *J. Appl. Meteorol. Climatol.* 50, 2267–2269.
- Sultana, R., Ahmed, Z., Hossain, M.A., Begum, B.A., 2021. Impact of green roof on human comfort level and carbon sequestration: a microclimatic and comparative assessment in Dhaka City, Bangladesh. *Urban Clim.* 38, 100878.

- Tabassum, A., Hong, S.-H., Park, K., Baik, J.-J., 2025. Simulating urban heat islands and local winds in the Dhaka metropolitan area, Bangladesh. *Urban Clim.* 59, 102284.
- Tabassum, A., Park, K., Seo, J.M., Han, J.-Y., Baik, J.-J., 2024. Characteristics of the urban heat island in Dhaka, Bangladesh, and its interaction with heat waves. *Asia-Pac. J. Atmos. Sci.* 60, 479–493.
- Touchaei, A.G., Akbari, H., Tessum, C.W., 2016. Effect of increasing urban albedo on meteorology and air quality of Montreal (Canada) – episodic simulation of heat wave in 2005. *Atmos. Environ.* 132, 188–206.
- UN-Habitat, 2022. World Cities Report 2022: Envisaging the Future of Cities. United Nations Human Settlements Programme, Nairobi, p. 387.
- Wang, X., Li, H., Sodoudi, S., 2022. The effectiveness of cool and green roofs in mitigating urban heat island and improving human thermal comfort. *Build. Environ.* 217, 109082.
- Wang, X., Liu, G., Zhang, N., Liu, H., Tang, X., Lyu, M., Meng, H., 2023. Effects of cooling roofs on mitigating the urban heat island and human thermal stress in the Pearl River Delta, China. *Build. Environ.* 245, 110880.
- WHO, 2021. WHO Global Air Quality Guidelines. Particulate Matter (PM<sub>2.5</sub> and PM<sub>10</sub>), Ozone, Nitrogen Dioxide, Sulfur Dioxide and Carbon Monoxide. World Health Organization, Geneva, p. 273.
- Zhang, J., Hu, D., 2024. The interaction of urban heat mitigation strategies-a case study in Beijing. *Urban Clim.* 56, 102089.
- Zhang, J., Li, Y., Tao, W., Liu, J., Levinson, R., Mohegh, A., Ban-Weiss, G., 2019. Investigating the urban air quality effects of cool walls and cool roofs in Southern California. *Environ. Sci. Technol.* 53, 7532–7542.
- Zhong, T., Zhang, N., Lv, M., 2021. A numerical study of the urban green roof and cool roof strategies' effects on boundary layer meteorology and ozone air quality in a megacity. *Atmos. Environ.* 264, 118702.